Extending the Stability Field of Polymeric Carbon Dioxide Phase V beyond the Earth's Geotherm

Demetrio Scelta
ICCOM-CNR, Institute of Chemistry of OrganoMetallic Compounds, National Research Council of Italy, Via Madonna del Piano 10, I-50019 Sesto Fiorentino, Firenze, Italy and LENS, European Laboratory for Non-linear Spectroscopy, Via N. Carrara 1, I-50019 Sesto Fiorentino, Firenze, Italy

Kamil F. Dziubek*
LENS, European Laboratory for Non-linear Spectroscopy, Via N. Carrara 1, I-50019 Sesto Fiorentino, Firenze, Italy

Martin Ende and Ronald Miletich
Institut für Mineralogie und Kristallographie, Universität Wien, Althanstrasse 14, A-1090 Wien, Austria

Mohamed Mezouar and Gaston Garbarino
European Synchrotron Radiation Facility, ESRF, 71 avenue des Martyrs, CS 40220, 38043 Grenoble Cedex 9, France

Roberto Bini
LENS, European Laboratory for Non-linear Spectroscopy, Via N. Carrara 1, I-50019 Sesto Fiorentino, Firenze, Italy; ICCOM-CNR, Institute of Chemistry of OrganoMetallic Compounds, National Research Council of Italy, Via Madonna del Piano 10, I-50019 Sesto Fiorentino, Firenze, Italy; and Dipartimento di Chimica "Ugo Schiff" dell'Università degli Studi di Firenze, Via della Lastruccia 3, I-50019 Sesto Fiorentino, Firenze, Italy

(Received 12 August 2020; revised 13 November 2020; accepted 11 December 2020)

We present a study on the phase stability of dense carbon dioxide (CO_2) at extreme pressure-temperature conditions, up to 6200 K within the pressure range 37 ± 9 to 106 ± 17 GPa. The investigations of high-pressure high-temperature *in situ* x-ray diffraction patterns recorded from laser-heated CO_2, as densified in diamond-anvil cells, consistently reproduced the exclusive formation of polymeric tetragonal CO_2-V at any condition achieved in repetitive laser-heating cycles. Using well-considered experimental arrangements, which prevent reactions with metal components of the pressure cells, annealing through laser heating was extended individually up to approximately 40 min per cycle in order to keep track of upcoming instabilities and changes with time. The results clearly exclude any decomposition of CO_2-V into the elements as previously suggested. Alterations of the Bragg peak distribution on Debye-Scherrer rings indicate grain coarsening at temperatures >4000 K, giving a glimpse of the possible extension of the stability of the polymeric solid phase.

DOI:

The exceptional stability of carbon dioxide (CO_2) makes it one of the most essential inorganic compounds. Its molecular form is the energetically lowest combination between the elemental constituents, carbon and oxygen, as found at the bottom of the composition-energy convex hull. As the CO_2 stoichiometry represents a true thermodynamic sink, the high bond enthalpy itself explains the high level of chemical inertness of CO_2, which in return is the background for its technical applicability (e.g., as nonreactive agent in fire extinguishers). This intuitive chemical view might require significant revision considering nonambient pressure conditions, where density is also a fundamental parameter determining the phase stability. Once the van der Waals space within the molecular solid is substantially compressed as intermolecular spacings get reduced, the initial hierarchy of electronic levels becomes perturbed. Shifting significant parts of the electron densities towards former intermolecular regions allows new chemical bonds to be formed, which in turn increase the effective coordination numbers [1,2]. This leads to a rearrangement of the bonding scheme in a manner resembling that of SiO_2, where tetrahedral configurations become the predominant primary building units of polymerlike structures [3]. Numerous molecular CO_2 phases have been recognized (see the recent review by Santoro *et al.* [4]) revealing rich polymorphism, including metastable states and transitions between them at comparably low energy barriers.

The solid-state polymerization, on the other hand, is much more difficult to accomplish and requires overcoming a substantial kinetic barrier [3]. Accordingly, the formation of an extended phase with polymerized tetrahedral units was achieved the first time through laser heating

in a diamond anvil cell (DAC) [5,6]. The experiments provided the synthesis of a stable crystalline polymeric phase of CO_2, known as phase V, whose structure was later determined as analogous to that of partially collapsed tetragonal β-cristobalite (space group $I\bar{4}2d$) [7,8]. This remarkable achievement was followed by suggestions of more complex polymorphism in the nonmolecular part of the phase diagram including extended phases with higher-coordinated carbon atoms (phase VI) [9] and an ionic crystal form (i-CO_2) [10]. However, other authors later disagreed with these findings, noting that all the other nonmolecular phases are kinetically trapped metastable states, as they all transform to phase V upon annealing [11]. The lack of *in situ* studies at extreme conditions (high pressure, high temperature) made it rather difficult to draw definite conclusions about equilibrium states and the transient character of the involved structures.

With respect to the physicochemical properties of CO_2, another puzzle is related to its chemical stability at extreme pressure-temperature (P-T) conditions. Several previous reports suggested that dense CO_2 disproportionates at high temperature and pressure yielding diamond and ϵ-oxygen as decomposition products [12–14]. In each of these studies the proposed reaction boundary has a pronounced negative slope in P-T space. Simple extrapolation of these reaction thresholds to higher pressures would be in striking contradiction to experimental results. In fact, they show the stability of CO_2-V upon further heating to at least 3000 K at $P > 40$ GPa [5], formation of i-CO_2 at 1700–1800 K and 85 GPa [10], or the exceptional stability of phase V at pressures exceeding even 100 GPa at temperatures up to 2700 K [15]. These discrepancies regarding the actual behavior of compressed carbon dioxide can be explained addressing reactions between CO_2 and metal gasket materials [16,17] or with the catalytic action exerted by the metals used as laser absorbers. Indeed, Litvin attributed the formation of diamond from CO_2 in static experiments to the reducing environment of the sample [18]. However, as densification usually suppresses molecularity and generally promotes the formation of extended structures, it might have been presumed that any dissociation line as reported in Ref. [12–14] should not extrapolate to high-pressure conditions. Moreover, it must be emphasized that none of the computational approaches supports the conjecture of CO_2 dissociation into elements, whereas the calculations predict a melting curve to exist between the solid CO_2-V and a liquid phase, being the molten phase presumably also polymeric [19–21]. In addition, calculations reveal that the enthalpy of the decomposition of CO_2-V into elements is relatively high and explain the presence of oxygen and diamond being due to experimental nonequilibrium conditions [22]. All the aforementioned ambiguities have not been tackled, from an experimental point of view, in a systematic way.

Here we report on *in situ* investigations by means of synchrotron XRD in a laser heated DAC at hot-spot temperatures (T_{HS}) up to 6200 K of a CO_2 sample compressed to pressures between 37 ± 9 and 106 ± 17 GPa. This experimental study is motivated by several objectives, i.e., (i) to prove whether CO_2-V is actually the thermodynamically stable phase in the investigated P-T range even beyond the temperatures previously reached; (ii) to prove the possible existence of any further stable structure in the P-T range beyond the conditions relevant to Earth's geotherm; (iii) to verify the mutual breakdown reaction, to track down its equilibrium boundary conditions in P-T space, and to check whether a possible recombination to CO_2 from dissociation products takes place on reducing the temperature; and (iv) to gain insights about the melting curve predicted from computational approaches within the experimental accessible P-T range.

The conflicting and partially contradicting results described in the introduction prompted us to pay particular attention to sample preparation. To this purpose, we tried to eliminate all the sources of side effects that could interfere with the transformation of the CO_2 sample. Therefore, one of the precautions was to avoid metal components that are expected to be somewhat reactive towards CO_2. This applies to the choice of the laser absorber material but also to the rhenium metal gasket which in particular has been reported to react with CO_2 at nonambient conditions [16]. Hence we decided to protect the interface at the pressure-chamber wall with a several micron thick gold coating, which is known to be completely inert to CO_2 at laser-heating conditions [16]. Moreover, as any of the conventionally used metallic laser-coupling materials can also react with the sample, we considered alternative coupling materials in connection with using a CO_2 laser. While CO_2-V is efficiently synthesized on heating with a CO_2 laser (10.6 μm) from dense carbonia at pressures <80 GPa [6], we have recently found that $MgCO_3$ is an excellent absorber even at higher pressures and its possible changes under high P-T conditions do not contaminate the sample [15]. In fact, the ν_2 in-plane bending and ν_4 out-of-plane bending active infrared modes of the CO_3^{2-} anion match very well with the CO_2 laser wavelength [23]. Fragments from a few-μm thick section of cryptocrystalline $MgCO_3$ (gelmagnesite) were placed inside the borehole of a Re gasket and protected by a 5–10 μm thick gold cover, which in turn also served as a pressure marker. CO_2, cryogenically liquefied at 23 bar, was loaded in a manner reported elsewhere [15]. All the other materials within the pressure chamber have been dispensed with, including conventional pressure sensors (e.g., ruby chips) or any thermal insulation layer.

In total, four cycles of laser heating were performed while keeping records on temperatures by means of pyrometry and on the time span of annealing at individual temperatures. *In situ* XRD patterns were collected in P-T space in the range 37 ± 9 and 106 ± 17 GPa and T_{HS} 2700 ± 150 and 6200 ± 150 K as shown in Fig. 1. Periods

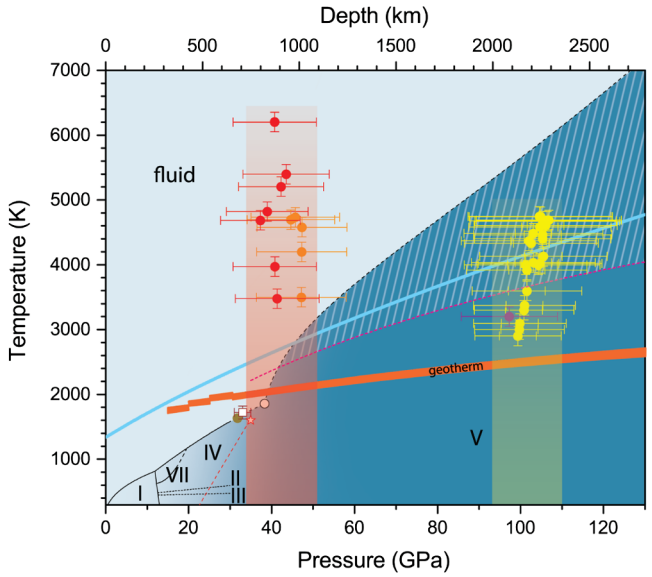

F1:1 FIG. 1. Overlap of the high-pressure and high-temperature
F1:2 phase diagrams, respectively, showing the stability fields of
F1:3 molecular (light blue) and extended (blue) liquid and solid
F1:4 phases of CO_2. The colors have been chosen in order to
F1:5 highlight the different chemical nature of the two systems.
F1:6 Except for those between phases III and II [9] and phases II and
F1:7 IV [34], indicated as dotted lines and likely referring to kinetic
F1:8 phases, experimentally defined melting lines or phase bounda-
F1:9 ries are indicated by solid lines, while dashed lines refer to
F1:10 computed or extrapolated curves. The blended region represents
F1:11 the *P*-*T* conditions where polymeric phase V can be quenched
F1:12 on decompression. All the reported phase boundaries are
F1:13 displayed according to literature data [9,34,35]. The reported
F1:14 boundary between molecular and extended phase V (red dashed
F1:15 line) follows the results of recent *ab initio* DFT calculations
F1:16 [36]. Very different computed melting lines were proposed for
F1:17 pressure above 35 GPa [19,21]. The reported melting line is
F1:18 following both experimental results (up to 30 GPa) [14,35,37]
F1:19 and computational data (for higher pressures) [20]; the striped
F1:20 area identifies the *P*,*T* region comprises between the higher [20]
F1:21 and the lower [21] computed melting curves for the polymeric
F1:22 phase (black and magenta dashed lines, respectively). The black
F1:23 open circle represents the triple point obtained as the inter-
F1:24 section of the higher temperature melting curve of phase V [20]
F1:25 and the extrapolation of the melting curve for CO_2-VII [35]. The
F1:26 triple point measured by Litasov [14], and those computed by
F1:27 Teweldeberhan [20] and Cogollo-Olivo [36], are also displayed
F1:28 as the wine open square, dark yellow full circle, and red open
F1:29 star, respectively. The full colored circles represent the indi-
F1:30 vidual data points acquired at T_{HS} during the four laser heating
F1:31 cycles (LH). Violet: LH1; yellow: LH2; orange: LH3; red: LH4.
F1:32 The rectangles highlight the *T* ranges explored during LH1-2
F1:33 (yellow) and LH3-4 (red). For each point the pressure was
F1:34 determined using the thermal equation of state of gold [38]
F1:35 employing the approach described in detail in the experimental
F1:36 section. The melting curve of gold is shown as a blue solid line
F1:37 [39]. Experimental data are summarized in the Supplemental
F1:38 Material (Table SI-1 [24]). The solid orange line corresponds to
F1:39 the adiabatic temperature profile of the Earth's mantle after
F1:40 Katsura *et al.* [40].

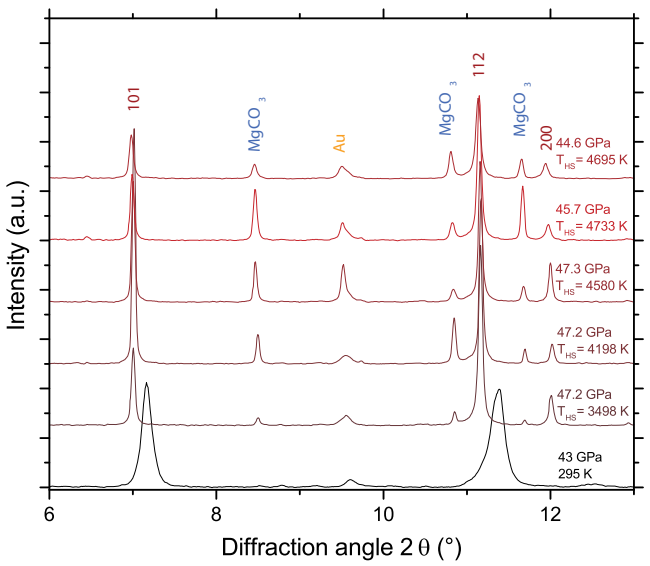

F2:1 FIG. 2. A selection of integrated XRD patterns from the third
F2:2 laser heating cycle, after appropriate background correction (from
F2:3 black, room *T*, to red, highest hot-spot temperatures T_{HS} in the
F2:4 displayed run). Diffraction peaks are labeled according to the
F2:5 assigned phases (i.e., CO_2-V, Au, $MgCO_3$). Further details,
F2:6 including the Le Bail fits, are provided in Fig. SI-1 [24].

of temperature annealing expand up to approximately 40 min per cycle in order to keep track of upcoming instabilities and to be able to record any changes with time, as due to kinetic sluggishness. This includes the possibilities of incomplete solid-solid transformations, the occurrence of transient states, the relaxation of stress, and the process of diffusion-controlled alterations, including crystal growth. The evaluation of XRD patterns reveals that after compression at room temperature the polymeric amorphous CO_2 transforms instantly to phase V on laser heating (cf. Fig. 2) [4], as already observed in previous experiments [15]. All patterns indicate the presence of solid CO_2-V as the only crystalline solid in the C-O system. All the remaining XRD features are related exclusively to Au metal and $MgCO_3$ (see Fig. SI-1 [24]). Integrated profile lines and diffraction patterns were carefully inspected for the presence of Bragg peaks of the potential breakdown products, i.e., ϵ-oxygen (and its relevant low-pressure forms), crystalline forms of carbon, carbon monoxide, and $MgCO_3$-II. All observed XRD maxima could be assigned to the known phases mentioned above. There is no evidence of a yet unknown polymorph or of a temporary transient state of an intermediate crystalline solid. The diffraction data attest for an excellent crystallinity of CO_2-V, increasing with raising the temperature, in line with the expected stress release upon exceptionally long annealing (cf. Fig. SI-2 [24]). In addition, the high crystallinity can be seen as a strong argument for the apparent stability of CO_2-V under these conditions, which would not be expected for a mutual transformation in

context with the suggested breakdown reaction. The evaluation of all patterns unanimously showed no evidence of a structural destabilization of CO_2-V, not at the highest temperature at 6200 K, nor after almost 40 min of continuous annealing at 4000–4700 K, reached at the hottest point of the sample.

These findings confirm the assumption previously reported that the formation of diamond and oxygen as products of the breakdown of CO_2 in laser-heated DAC experiments can be plausibly attributed to the redox reaction with the gasket [18]. Here in this study we successfully implemented a protective layer of inert Au at the interface between the gasket and the hot CO_2 sample that actually could not react as it did in the majority of previous DAC experiments [16,17]. This proof of existence of cristobalite-type CO_2-V as a phase being stable and not undergoing disproportionation means that solid CO_2 can theoretically occur not only under the conditions of the Earth's geotherm, but even under far more extreme conditions. With respect to the discussion of the diamond formation in the Earth's mantle [33], it confirms that for depths larger than 1000 km this polymeric form would occur as an equilibrium component within the Earth's mantle, as long as it does not react away with reducing components of the planetary interior, i.e., Fe^{2+} oxides and silicates, or iron-bearing alloys.

After quenching, the samples were further characterized at room temperature by XRD measuring a mesh of 40 μm^2 across the entire sample chamber. This procedure was mandatory in order to check profiles across the pressure chamber as existing P and T gradients might be responsible for differences, but also to record possible reactions in the marginal areas at the interface with the pressure-chamber wall. Profiling across this mesh reveals a consistent picture of exclusively those phases reported before. There was no evidence of any decomposition products, nor of reaction products with the gasket material. Moreover, the measurements performed on the quenched sample successively decompressed stepwise from 106 GPa provided valuable crystallographic data on the isothermal lattice evolution at static pressure conditions. This is of particular interest since decompression of CO_2-V from 120 down to 90 GPa showed a negative linear compressibility for the tetragonal c-axis direction [15] that compared with previous studies suggested the presence of a maximum for this parameter between 40 and 90 GPa. Although we managed to decompress the sample down to ~20 GPa, only the data above 58 GPa appear to be of sufficient quality (see also Fig. SI-3 [24]). This is due to the increasingly strong deviatoric stress induced in the sample in absence of a suitable hydrostatic pressure transmitting medium (PTM) during decompression. It needs to be emphasized that the data collected for annealed samples, preferably embedded in a PTM, would expectedly be less scattered, setting the direction for future research. With this reservation in mind, based on Le Bail fits of the diffraction profile lines, it can be concluded that the pressure dependence of the lattice parameter c has a maximum around ~90 GPa (Fig. 3), thus confirming the findings and trend lines reported in previous studies [15] and showing a negative compressibility along the c-axis lattice direction at least between ~30 and ~90 GPa. This finding corroborates with an earlier supposition of the existence of a maximum in the c parameter-pressure relationship [15], at the same time implying a consistent anisotropic distortion of the tetrahedra possibly related to the preferential arrangement of the crystallites with respect to the compression direction. The latter issue could also explain the variability of the absolute values of this parameter in different experiments. Moreover, the new data obtained for the unit-cell volume match very well with the EOS calculated in our previous study in the megabar range, with respect to a simple extrapolation of the EOS determined earlier based on the data collected up to ~65 GPa [8] (for details, cf. Fig. 3).

As far as melting is concerned, we did not get clear indications of proper melt formation. All recorded patterns are dominated by the diffraction features of crystalline CO_2-V. This applies to the highest temperatures reached, where we only observed the progressive transformation of the Debye-Scherrer rings of phase V to an extremely rich spotty appearance related to the reflections of individual microcrystalline grains (see 2D diffraction images in Fig. SI-2 and Fig. SI-4 [24]).

To carefully discuss possible interpretation scenarios of our experimental observations, one should take into account the measurement conditions and instrumental settings. In the experimental setup, the hot spot of the CO_2 laser has a focal depth below 100 μm and a FWHM of approximately 25 μm but no specific characterization of the temperature profile within the focal spot, as instead is known for the YAG laser [42], is available. Furthermore, it needs to be emphasized that both CO_2 and $MgCO_3$ have poor thermal conductivity and in the absence of insulation layers one can assume that the heat dissipates mostly through the diamond anvils which are an excellent heat sink. The DAC was carefully centered before each laser heating cycle using a standard procedure [43]. The diameter of the borehole at experimental conditions was not larger than ~40 μm. The primary x-ray beam was focused down to an approximate diameter of ~3 μm by one pair of Kirkpatrick-Baez mirrors and additionally cleaned by a pinhole. The laser and the x-ray microbeam were aligned following a protocol reported by Mezouar *et al.* [42]. Nevertheless, in almost all recorded 2D images, weak yet noticeable diffraction lines coming from the gold lining of the gasket were visible. Moreover, their relative intensity slowly increased with laser heating duration to the point at which realignments of the pinhole were necessary. The Au reflections were barely visible only in the first image recorded after this intervention, but again they began to gradually increase in intensity from this point

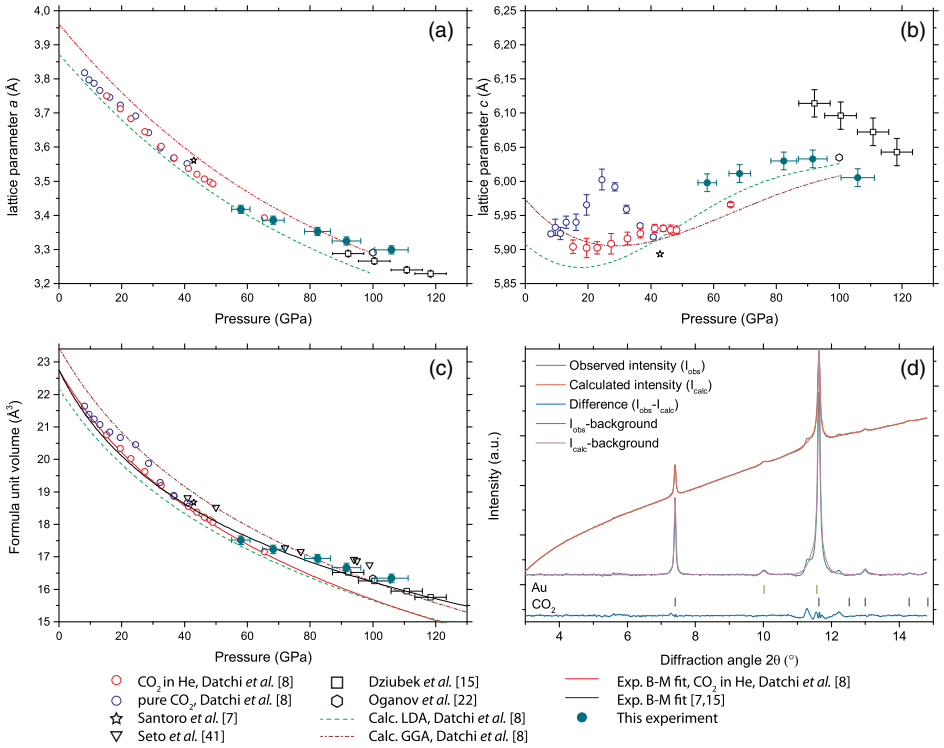

F3:1 FIG. 3. Crystallographic lattice parameters of CO_2-V and their evolution with pressure: tetragonal lattice parameters a and c [(a) and
F3:2 (b)]; formula unit volume (c); and an example of the Le Bail fit of the XRD profile at 106 GPa and room temperature (d): here, the
F3:3 unassigned weak features observed on both shoulders of the CO_2-V 112 line can be explained by intracrystalline strain gradients
F3:4 (cf. Fig. 2 in Ref. [15]). The error bars represent the uncertainties of lattice parameters and volume as obtained from the profile fitting,
F3:5 while those for pressure correspond to $\pm 5\%$ relative uncertainties.

onward. Assuming that the DAC remained centered, this phenomenon can be rationalized by considering that the extended tails of the incident x-ray beam reach the gold coating. While the Au atom is a much stronger x-ray scatterer than C and O atoms, in these conditions the incident beam also illuminates areas of the specimen surrounding the hot spot where the temperature is lower and the solid CO_2-V inevitably occurs. Besides, presuming the 30–35 μm initial thickness of the gasket and a few μm thick layer of gelmagnesite (the laser coupler), the CO_2 melt zone may propagate at a certain distance from the $MgCO_3$ substrate attached to one of the diamonds, but does not necessarily reach the other culet surface (see Fig. SI-5 [24]). The observed time-dependent variation in granularity of the Debye-Scherrer rings, where the single-crystal spots appear and disappear as a function of time (as shown in Fig. SI-4 [24]), can also be explained if one suspects that the x-ray irradiated sample volume actually comprises both solid and molten fractions with dynamic crystallization ongoing at the interface. While an evident diffuse XRD signal corresponding to the liquid (which is often considered an outright melting criterion) is not visible in the recorded detector images, its absence can be accounted for essentially by the poor scattering power of low Z elements and the weak diffraction from noncrystalline materials in general.

With regard to all the aforementioned assumptions, it cannot be unambiguously concluded whether the melting conditions were reached in the course of the experiment. If not, the previously established computed melting line [19,20] is challenged by this measurement. However, if partial melting was achieved, it needs to be emphasized that even after prolonged laser heating we have not seen any evidence of carbon dioxide decomposition, i.e., diamond and oxygen among the products, thus letting us foresee the existence of a polymeric fluid. This second hypothesis appears more plausible, also considering the grain coarsening observed in Fig. SI-2 and Fig. SI-4 [24], which corroborates with the partial melting. This is in striking contrast with the previous studies [12–14] and still leaves unanswered the question of if the decomposition should be related to the melting of CO_2-V. In any of these two cases, the findings presented in this report are an important starting point in understanding the behavior of hot dense CO_2 and should stimulate further experimental studies of this substance in extreme pressure and temperature conditions.

The authors thank the Deep Carbon Observatory initiative (Extreme Physics and Chemistry of Carbon: Forms, Transformations, and Movements in Planetary Interiors, from the Alfred P. Sloan Foundation) that supported this

work. The authors also thank the ESRF ID-27 beam line scientific staff, the ESRF Sample Environment Support Service and particularly J. Jacobs for provision of a loan pool diamond anvil cell and Dr. Harald Müller of the ESRF Chemistry Laboratory for his help with sample loading. We are grateful to Andreas Wagner (University of Vienna) for the preparation of the gelmagnesite thin section. The authors are indebted to the anonymous referees for very helpful comments and suggestions.

*dziubek@lens.unifi.it

[1] C. T. Prewitt and R. T. Downs, High-pressure crystal chemistry, Rev. Mineral. Geochem. **37**, 283 (1998).

[2] W. Grochala, R. Hoffmann, J. Feng, and N. Ashcroft, The chemical imagination at work in very tight places, Angew. Chem. Int. Ed. **46**, 3620 (2007).

[3] M. Santoro, F. A. Gorelli, R. Bini, G. Ruocco, S. Scandolo, and W. A. Crichton, Amorphous silica-like carbon dioxide, Nature (London) **441**, 857 (2006).

[4] M. Santoro, F. A. Gorelli, K. Dziubek, D. Scelta, and R. Bini, Structural and chemical modifications of carbon dioxide on moving to deep earth, in *Carbon in Earth's Interior, Geophysical Monograph Series*, edited by C. Manning and W. Mao (American Geophysical Union, Washington, DC, USA, 2020).

[5] V. Iota, C. S. Yoo, and H. Cynn, Quartzlike carbon dioxide: An optically nonlinear extended solid at high pressures and temperatures, Science **283**, 1510 (1999).

[6] C. S. Yoo, H. Cynn, F. Gygi, G. Galli, V. Iota, M. Nicol, S. Carlson, D. Häusermann, and C. Mailhiot, Crystal Structure of Carbon Dioxide at High Pressure: "Superhard" Polymeric Carbon Dioxide, Phys. Rev. Lett. **83**, 5527 (1999).

[7] M. Santoro, F. A. Gorelli, R. Bini, J. Haines, O. Cambon, C. Levelut, J. A. Montoya, and S. Scandolo, Partially collapsed cristobalite structure in the non molecular phase V in CO_2, Proc. Natl. Acad. Sci. U.S.A. **109**, 5176 (2012).

[8] F. Datchi, B. Mallick, A. Salamat, and S. Ninet, Structure of Polymeric Carbon Dioxide CO_2-V, Phys. Rev. Lett. **108**, 125701 (2012).

[9] V. Iota, C.-S. Yoo, J.-H. Klepeis, Z. Jenei, W. Evans, and H. Cynn, Six-fold coordinated carbon dioxide VI, Nat. Mater. **6**, 34 (2007).

[10] C.-S. Yoo, A. Sengupta, and M. Kim, Carbon dioxide carbonates in the Earth's mantle: Implications to the deep carbon cycle, Angew. Chem. Int. Ed. **50**, 11219 (2011).

[11] F. Datchi and G. Weck, X-ray crystallography of simple molecular solids up to megabar pressures: Application to solid oxygen and carbon dioxide, Z. Krist.- Cryst. Mater. **229**, 135 (2014).

[12] O. Tschauner, H.-k. Mao, and R. J. Hemley, New Transformations of CO_2 at High Pressures and Temperatures, Phys. Rev. Lett. **87**, 075701 (2001).

[13] Y. Seto, D. Hamane, T. Nagai, and K. Fujino, Fate of carbonates within oceanic plates subducted to the lower mantle, and a possible mechanism of diamond formation, Phys. Chem. Miner. **35**, 223 (2008).

[14] K. D. Litasov, A. F. Goncharov, and R. J. Hemley, Crossover from melting to dissociation of CO_2 under pressure: Implications for the lower mantle, Earth Planet. Sci. Lett. **309**, 318 (2011).

[15] K. F. Dziubek, M. Ende, D. Scelta, R. Bini, M. Mezouar, G. Garbarino, and R. Miletich, Crystalline polymeric carbon dioxide stable at megabar pressures, Nat. Commun. **9**, 3148 (2018).

[16] D. Santamaría-Pérez, C. McGuire, A. Makhluf, A. Kavner, R. Chuliá-Jordán, J. Pellicer-Porres, D. Martinez-García, A. Doran, M. Kunz, P. Rodríguez-Hernández, and A. Muñoz, Exploring the chemical reactivity between carbon dioxide and three transition metals (Au, Pt, and Re) at high-pressure, high-temperature conditions, Inorg. Chem. **55**, 10793 (2016).

[17] R. Chuliá-Jordán, D. Santamaría-Pérez, T. Marqueño, J. Ruiz-Fuertes, and D. Daisenberger, Oxidation of high yield strength metals tungsten and rhenium in high-pressure high-temperature experiments of carbon dioxide and carbonates, Crystals **9**, 676 (2019).

[18] Y. A. Litvin, *Genesis of Diamonds and Associated Phases* (Springer International Publishing, 2017).

[19] B. Boates, A. M. Teweldeberhan, and S. A. Bonev, Stability of dense liquid carbon dioxide, Proc. Natl. Acad. Sci. U.S.A. **109**, 14808 (2012).

[20] A. Teweldeberhan, B. Boates, and S. Bonev, CO_2 in the mantle: Melting and solid-solid phase boundaries, Earth Planet. Sci. Lett. **373**, 228 (2013).

[21] C. J. Wu, D. A. Young, P. A. Sterne, and P. C. Myint, Equation of state for a chemically dissociative, polyatomic system: Carbon dioxide, J. Chem. Phys. **151**, 224505 (2019).

[22] A. R. Oganov, S. Ono, Y. Ma, C. W. Glass, and A. Garcia, Novel high-pressure structures of $MgCO_3$, $CaCO_3$ and CO_2 and their role in Earth's lower mantle, Earth Planet. Sci. Lett. **273**, 38 (2008).

[23] J. Santillán, K. Catalli, and Q. Williams, An infrared study of carbon-oxygen bonding in magnesite to 60 GPa, Am. Mineral. **90**, 1669 (2005).

[24] See Supplemental Material at http://link.aps.org/supplemental/10.1103/PhysRevLett.000.000000 for further details on the methods used in the study, additional figures and numerical data. Supplemental Material also includes Refs. [25–32].

[25] S. Anzellini, A. Dewaele, F. Occelli, P. Loubeyre, and M. Mezouar, Equation of state of rhenium and application for ultra high pressure calibration, J. Appl. Phys. **115**, 043511 (2014).

[26] G. Ashiotis, A. Deschildre, Z. Nawaz, J. P. Wright, D. Karkoulis, F. E. Picca, and J. Kieffer, The fast azimuthal integration PYTHON library: pyFAI, J. Appl. Crystallogr. **48**, 510 (2015).

[27] C. Prescher and V. B. Prakapenka, Dioptas: A program for reduction of two-dimensional x-ray diffraction data and data exploration, High Press. Res. **35**, 223 (2015).

[28] V. Petříček, M. Dušek, and L. Palatinus, Crystallographic computing system JANA2006: General features, Z. Krist.- Cryst. Mater. **229**, 345 (2014).

[29] G. Morard, D. Andrault, N. Guignot, C. Sanloup, M. Mezouar, S. Petitgirard, and G. Fiquet, In situ determination of Fe − sbFe_3S phase diagram and liquid structural properties up to 65 GPa, Earth Planet. Sci. Lett. **272**, 620 (2008).

[30] N. A. Solopova, L. Dubrovinsky, A. V. Spivak, Y. A. Litvin, and N. Dubrovinskaia, Melting and decomposition of $MgCO_3$ at pressures up to 84 GPa, Phys. Chem. Miner. **42**, 73 (2015).

[31] G. Fiquet, F. Guyot, M. Kunz, J. Matas, D. Andrault, and M. Hanfland, Structural refinements of magnesite at very high pressure, Am. Mineral. **87**, 1261 (2002).

[32] J. Binck, L. Bayarjargal, S. S. Lobanov, W. Morgenroth, R. Luchitskaia, C. J. Pickard, V. Milman, K. Refson, D. B. Jochym, P. Byrne, and B. Winkler, Phase stabilities of $MgCO_3$ and $MgCO_3$-II studied by Raman spectroscopy, x-ray diffraction, and density functional theory calculations, Phys. Rev. Mater. **4**, 055001 (2020).

[33] S. B. Shirey, K. V. Smit, D. G. Pearson, M. J. Walter, S. Aulbach, F. E. Brenker, H. Bureau, A. D. Burnham, P. Cartigny, T. Chacko *et al.*, Diamonds and the mantle geodynamics of carbon: Deep mantle carbon evolution from the diamond record, in *Deep Carbon: Past to Present*, edited by B. N. Orcutt, I. Daniel, and R. Dasgupta (Cambridge University Press, Cambridge, England, 2019), pp. 89–128.

[34] V. Iota and C.-S. Yoo, Phase Diagram of Carbon Dioxide: Evidence for a New Associated Phase, Phys. Rev. Lett. **86**, 5922 (2001).

[35] V. M. Giordano and F. Datchi, Molecular carbon dioxide at high pressure and high temperature, Europhys. Lett. **77**, 46002 (2007).

[36] B. H. Cogollo-Olivo, S. Biswas, S. Scandolo, and J. A. Montoya, Ab Initio Determination of the Phase Diagram of CO_2 at High Pressures and Temperatures, Phys. Rev. Lett. **124**, 095701 (2020).

[37] V. M. Giordano, F. Datchi, and A. Dewaele, Melting curve and fluid equation of state of carbon dioxide at high pressure and high temperature, J. Chem. Phys. **125**, 054504 (2006).

[38] Y. Fei, A. Ricolleau, M. Frank, K. Mibe, G. Shen, and V. Prakapenka, Toward an internally consistent pressure scale, Proc. Natl. Acad. Sci. U.S.A. **104**, 9182 (2007).

[39] G. Weck, V. Recoules, J.-A. Queyroux, F. Datchi, J. Bouchet, S. Ninet, G. Garbarino, M. Mezouar, and P. Loubeyre, Determination of the melting curve of gold up to 110 GPa, Phys. Rev. B **101**, 014106 (2020).

[40] T. Katsura, A. Yoneda, D. Yamazaki, T. Yoshino, and E. Ito, Adiabatic temperature profile in the mantle, Phys. Earth Planet. Inter. **183**, 212 (2010).

[41] Y. Seto, D. Nishio-Hamane, T. Nagai, N. Sata, and K. Fujino, Synchrotron x-ray diffraction study for crystal structure of solid carbon dioxide CO_2-V, J. Phys. Conf. Ser. **215**, 012015 (2010).

[42] M. Mezouar, R. Giampaoli, G. Garbarino, I. Kantor, A. Dewaele, G. Weck, S. Boccato, V. Svitlyk, A. D. Rosa, R. Torchio, O. Mathon, O. Hignette, and S. Bauchau, Methodology for *in situ* synchrotron x-ray studies in the laser-heated diamond anvil cell, High Press. Res. **37**, 170 (2017).

[43] J. S. Smith and S. Desgreniers, Selected techniques in diamond anvil cell crystallography: Centring samples using x-ray transmission and rocking powder samples to improve x-ray diffraction image quality, J. Synchrotron Radiat. **16**, 83 (2009).